JOURNAL OF ENVIRONMENTAL SCIENCES 32 (2015) 102–107

Available online at www.sciencedirect.com

ScienceDirect

www.journals.elsevier.com/journal-of-environmental-sciences

JOURNAL OF ENVIRONMENTAL SCIENCES

www.jesc.ac.cn

Cu–Mn–Ce ternary mixed-oxide catalysts for catalytic combustion of toluene

Hanfeng Lu[1,*], *Xianxian Kong*[2], *Haifeng Huang*[2], *Ying Zhou*[1], *Yinfei Chen*[1,*]

1. *Institute of Catalytic Reaction Engineering, College of Chemical Engineering, Zhejiang University of Technology, Hangzhou 310014, China. E-mail:* luhf@zjut.edu.cn

2. *College of Biological and Environmental Engineering, Zhejiang University of Technology, Hangzhou 310014, China*

ARTICLE INFO

Article history:
Received 30 August 2014
Revised 28 October 2014
Accepted 13 November 2014
Available online 24 April 2015

Keywords:
Cu–Mn–Ce mixed oxide
Toluene
Catalytic combustion
Volatile organic compounds (VOCs)

ABSTRACT

Cu–Mn, Cu–Mn–Ce, and Cu–Ce mixed-oxide catalysts were prepared by a citric acid sol–gel method and then characterized by XRD, BET, H_2-TPR and XPS analyses. Their catalytic properties were investigated in the toluene combustion reaction. Results showed that the Cu–Mn–Ce ternary mixed-oxide catalyst with 1:2:4 mole ratios had the highest catalytic activity, and 99% toluene conversion was achieved at temperatures below 220°C. In the Cu–Mn–Ce catalyst, a portion of Cu and Mn species entered into the CeO_2 fluorite lattice, which led to the formation of a ceria-based solid solution. Excess Cu and Mn oxides existed on the surface of the ceria-based solid solution. The coexistence of Cu–Mn mixed oxides and the ceria-based solid solution resulted in a better synergetic interaction than the Cu–Mn and Cu–Ce catalysts, which promoted catalyst reducibility, increased oxygen mobility, and enhanced the formation of abundant active oxygen species.

Introduction

Volatile organic compounds (VOCs) are some of the most harmful air pollutants because they are acutely toxic toward the environment and humans (Parmar and Rao, 2009). Among various available techniques, catalytic combustion is an effective and widely applied technology for the abatement of VOCs (Everaert and Baeyens, 2004). The low operating temperature and high efficiency of this technology has led to considerable environmental and economic benefits, as well as application in the field of industrial emission (Huang et al., 2008; Lu et al., 2011). The catalysts most commonly used in the combustion of VOCs are of two types, namely, those based on noble metals and metal mixed oxides. Noble metal catalysts are widely used in the catalytic combustion of VOCs (Okumura et al., 2003; Saqer et al., 2009). However, in addition to the high cost of noble metal catalysts, they are susceptible to poisons such as impurities in the feed stream or intermediates formed during oxidation (Zhao et al., 2010). Thus, intensive efforts are being directed toward the design and synthesis of catalytic materials based on metal oxides as a substitute for noble metal catalysts (Lu et al., 2013a, 2013b). Manganese and copper mixed oxides are considered highly active and promising catalysts for the combustion of VOCs (Morales et al., 2006; Zimowska et al., 2007). Morales et al. (2006) prepared stable crystalline-phase mixed MnO_χ and CuO catalysts by coprecipitation, and investigated their performance in ethanol and propane catalytic combustion. They found that the catalyst activity was generally as good as that of noble metal catalysts, such as those based on platinum and palladium (Du et al., 2008; Morales et al., 2009).

The $CuMn_2O_4$ spinel oxide structure is considered the main active phase in Cu–Mn catalysts. However, the $CuMn_2O_4$ structure easily decomposes into $Cu_\chi Mn_{3-\chi}O_4$ (χ = 1.4–1.6)

* *Corresponding authors*. E-mail: yfchen@zjut.edu.cn (Y. Chen).

http://dx.doi.org/10.1016/j.jes.2014.11.015
1001-0742/

and Mn_2O_3 or Mn_3O_4 at high temperature (Tanaka et al., 2005). In a sense, $Cu_{1.5}Mn_{1.5}O_4$ is the real active phase. Hutchings et al. (1998) also proved that the $Cu_{1.5}Mn_{1.5}O_4$ and MnO_x mixed structure is the main active site in Cu-Mn composite oxide catalysts during CO oxidation. Even in the methanol steam-reforming reaction, Papavasiliou et al. (2006, 2007) also considered that $Cu_xMn_{3-x}O_4$ spinel oxide and MnO_x are the main active phases. In summary, the presence of such a mixed structure of $Cu_{1.5}Mn_{1.5}O_4$ and MnO_x plays an important role in the catalytic oxidation of VOCs over Cu–Mn-based catalysts. $Cu_{1.5}Mn_{1.5}O_4$ is the active site, whereas MnO_x is the center of oxygen supply and transmission for providing $Cu_{1.5}Mn_{1.5}O_4$ with active oxygen to completely oxidize organic molecules.

Based on the abovementioned active structure model, we believe that if other metal oxides with better oxygen-supply capacity and oxygen storage capacity are used to replace MnO_x, the activity of Cu–Mn catalysts can be further promoted. CeO_2 is known to have excellent oxygen storage capacity and is widely used in the field of catalytic oxidation (Wang et al., 2008; Lu et al., 2013a). Therefore, using Ce as a partial substitute for Mn in Cu–Mn catalysts can enable the preparation of catalysts with better oxygen capacity and higher performance for the catalytic oxidation of toluene.

In the present work, a series of Cu, Mn, and Ce mixed oxides with different Cu/Mn/Ce ratios was prepared and characterized by X-ray diffraction (XRD), Brunauer–Emmett–Teller (BET), H_2-temperature programmed reduction (TPR), and X-ray photoelectron spectroscopy (XPS) analyses. Their catalytic activities were evaluated in the catalytic combustion of toluene. The reaction mechanisms and structural features of these mixed-oxide catalysts were also discussed.

1. Experimental

1.1. Catalyst preparation

Mixed-oxide catalysts were prepared by a citric acid sol–gel method with appropriate amounts of Cu, Mn, and Ce nitrates as precursors. Copper nitrate, manganese nitrate, and cerium nitrate were mixed in appropriate molar ratios in an appropriate volume of distilled water to obtain a transparent solution (1.0 mol/L metal ion concentration). Then citric acid equimolar to the metal nitrates was added to the nitrate solution. The resulting solution was stirred and dried at 110°C overnight to form a solid gel. This gel was then calcined at 500°C for 3 hr. The obtained samples were ground, pelletized, and sieved to between 20 and 30 mesh size. The synthesized catalysts are hereafter denoted as $Cu_xMn_yCe_z$, where x:y:z represents the different Cu:Mn:Ce molar ratios. For comparison, samples of CuO, MnO_x, and CeO_2 were also prepared by the same method.

1.2. Catalyst characterization

1.2.1. BET specific surface area

The specific surface area of the catalysts was measured by the BET method from nitrogen adsorption isotherms. Experiments were carried out on a Micromeritics ASAP 2020 instrument at 77 K. Prior to experiments, samples were degassed at 427 K for 3 hr.

1.2.2. X-ray diffraction (XRD)

XRD data of the samples were collected on a SCINTAG XTRA X-ray diffractometer equipped with Ni-filtered Cu Kα (λ = 1.542 Å, 40 kV) radiation. The measurements were conducted within the 2θ range of 10°–60° with a step size of 0.033°.

1.2.3. Temperature programmed reduction (TPR)

TPR experiments were performed on a Autochem 3010E (Zhejiang Fine-Tech Instruments, China). A desired amount of sample (200 mg) was placed in a quartz reactor, pretreated in a flow of Ar gas at 250°C for 2 hr, and cooled to 70°C. A gas mixture of H_2 (5%) and Ar (95%) was then passed (30 mL/min) through the reactor. The temperature was increased from 70°C to 750°C at a heating rate of 10°C/min. A TCD detector was used at the outlet of the reactor to measure the volume of hydrogen consumed during reduction.

1.2.4. X-ray photoelectron spectroscopy (XPS)

A Kratos AXIS Ultra DLD photoelectron spectrometer with a monochromatized microfocused Al X-ray source was used for XPS measurements (Shimadzu scientific instruments, Japan). The charging of samples was corrected by setting the binding energy of adventitious carbon (C 1s) at 284.6 eV. Prior to measurements, the powdered samples were pressed into self-supporting disks, loaded into a sub-chamber, and then evacuated at 25°C for 4 hr.

1.3. Catalytic activity measurement

Catalytic combustion of toluene was conducted in a fixed-bed quartz tube reactor (10 mm i.d.) at atmospheric pressure. About 500 mg of catalyst mixed 1.5 g quartz sand was packed at the isothermal zone of the reactor. Gaseous VOCs were generated by flowing air from a mass-flow controller through liquid organics in an incubator placed in an ice bath. The VOC-containing stream was mixed with the main air stream introduced through another mass-flow controller. The feed (5.0 g/m^3 toluene in air) was introduced to the catalyst at a flow rate of 200 mL/min (gas hourly space velocity = 24,000 mL/(hr(gcat.))). The reactor effluent was analyzed online at desired temperatures with an HP 6890 gas chromatography system equipped with a flame ionization detector.

2. Results and discussions

2.1. Activity test

Morales et al. (2006) and Papavasiliou et al. (2007) confirmed that interactions among Cu–Mn oxides promote the activation of lattice oxygen, decrease the light-off temperature, and increase the dispersion of the active species. The selectivity to CO_2 also increases with increased Mn proportion. Many studies (Zimowska et al., 2007; Du et al., 2008; Morales et al., 2008) have shown that Cu_xMn_{1-x} (x = 0.1–0.3) catalysts

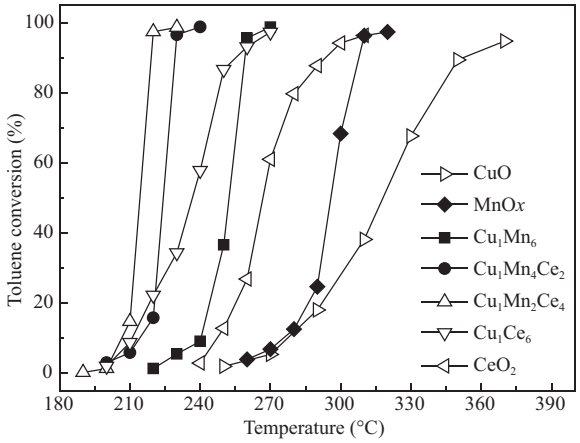

Fig. 1 – Light-off curves of toluene combustion over Cu–Mn–Ce mixed-oxide catalysts. Conditions: GHSV = 24,000 mL/(hr(gcat.)), toluene concentration: 5 g/m^3.

possess excellent catalytic performance, especially for the combustion of oxygen-containing organic compounds (*e.g.*, ethyl acetate, ethanol, acetone, *etc.*). These catalysts show strong oxidation ability, high selectivity toward CO_2, and even better catalytic performance than noble metals. Therefore, Cu_1Mn_6 was used in the current research as a Cu-Mn mixed-oxide catalyst model, and on this basis, Ce was used to partially substitute for Mn.

Fig. 1 shows the light-off curves of toluene combustion over Cu–Mn, Cu–Mn–Ce, and Cu–Ce catalysts. The activity of Cu–Mn–Ce ternary mixed-oxide catalysts is higher than those of Cu–Mn and Cu–Ce mixed-oxide catalysts. The performance of pure oxides (CuO, CeO_2, and MnO_x) in the total oxidation of toluene is lower than those of the mixed oxides. Complete toluene combustion occurs at 320°C over MnO_x catalysts, and 99% toluene combustion occurs at 270°C over the Cu_1Mn_6 catalyst. With the partial substitution of Mn by Ce, the activity of Cu–Mn–Ce catalysts is promoted, and the conversion curves shift to a much lower temperature. Both $Cu_1Mn_4Ce_2$ and $Cu_1Mn_2Ce_4$ appear to be superior for toluene catalytic combustion, which reaches 99.0% conversion when the reaction proceeds at about 230 and 220°C, respectively. This result is similar to those for conventional noble metal catalysts, such as Pd (Schwartz and Pfefferle, 2012) and Pt (Saqer et al., 2009). The experimental results in Fig. 2 indicate that T_{50} and T_{90} (where 50% and 90% conversions are reached) gradually decrease with Ce/(Cu + Mn + Ce) ratio from 0 to 0.57. However, the catalytic activity declines when Ce completely replaces Mn. This indicates that Mn ion is an essential element in the catalyst active phase during toluene combustion.

2.2. Texture characterization of catalysts

To gain a deep insight into the structural evolution, XRD patterns of the catalysts were measured and are shown in Fig. 3. The diffraction peaks of the Cu_1Mn_6 catalyst mainly correspond to the $Cu_{1.5}Mn_{1.5}O_4$ and Mn_3O_4 phases, which is different from catalysts prepared by coprecipitation (mainly Mn_2O_3 crystal phase) (Morales et al., 2008). The XRD patterns of $Cu_1Mn_2Ce_4$ and Cu_1Ce_6 catalysts show a single CeO_2 phase. No Cu and Mn oxide phases are found in the XRD patterns of the catalysts, indicating that a ceria-based solid solution structure is formed by the doping of Cu and Mn ions. Comparison of the XRD patterns of pure CeO_2 and $Cu_1Mn_2Ce_4$ catalysts reveals a decrease in the lattice parameter of Cu–Mn–Ce catalysts. In the $Cu_1Mn_2Ce_4$ sample, the cell constant declines from 0.5410 to 0.5364 nm, indicating that ceria-based solid solutions are formed by partial replacement of Ce^{4+} with these transition metal cations. Because the Mn^{4+}, Mn^{3+}, Cu^{2+}, and Cu^{+} ionic radii are 0.056, 0.062, 0.073, and 0.077 nm, respectively, which are all less than that of Ce^{4+} (0.097 nm), the lattice constant decreases on substitution.

Liang et al. (2008) and Tang et al. (2008) proved that when the Ce content is more than 50% in Cu–Ce and Mn–Ce catalysts, a solid solution of CeO_2 is easily formed. However, a solubility limit for Cu and Mn cations in CeO_2 was reported by Aranda et al. (2012) and Kang et al. (2006). The limit of Cu doping in the CeO_2 lattice is less than 14%, and that of Mn is about 5 mol% to 10 mol%, and highly depends on the preparation procedure. In the $Cu_1Mn_2Ce_4$ catalyst, the Cu and Mn contents are 14.3 mol% and 28.6 mol%, respectively.

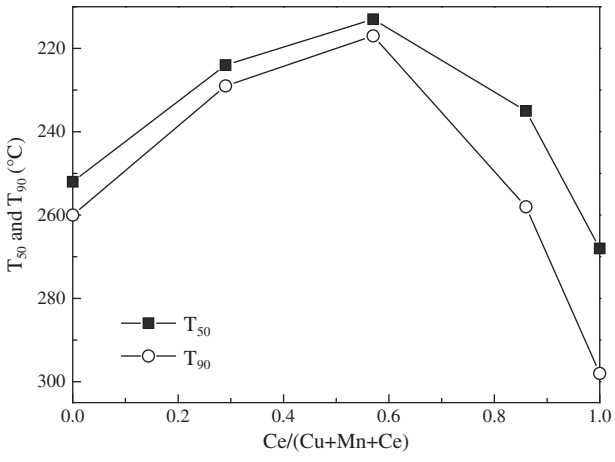

Fig. 2 – T_{50} and T_{90} of Cu–Mn–Ce ternary mixed-oxide catalysts for toluene combustion.

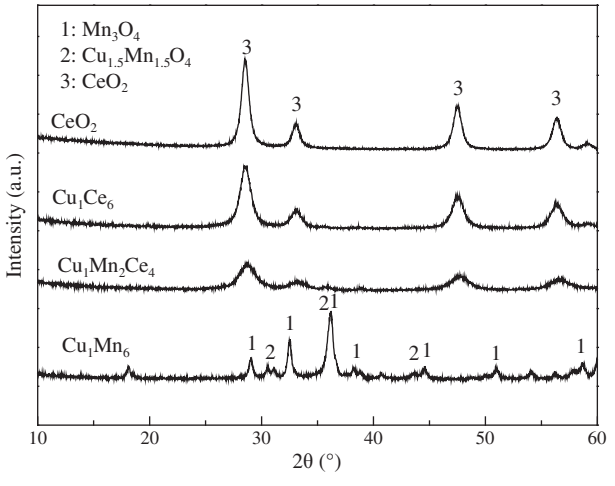

Fig. 3 – XRD patterns of CeO_2, Cu_1Mn_6, Cu_1Ce_6 and $Cu_1Mn_2Ce_4$ mixed-oxide catalysts.

Table 1 – Crystal structure and specific surface area of catalysts.

Samples	BET surface (m^2/g)	XLBA size (nm)	Cell (CeO_2) (a/nm)	Reduction temperature (°C)		H_2 consumption (mmol/g)
				T_1	T_2	
Cu_1Mn_6	37.9	12.5	/	200	280	5.72
$Cu_1Mn_2Ce_4$	45.3	5.80	0.5364	180	/	2.32
Cu_1Ce_6	68.3	7.30	0.5400	150	/	1.93
CeO_2	62.0	10.2	0.5410	520	/	2.66

Excess Cu and Mn in the $Cu_1Mn_2Ce_4$ catalysts may be highly dispersed on the surface of CeO_2 as CuO_X, MnO_X, or their mixed oxides. The crystalline structure, particle size, and morphology of the catalysts were also investigated by TEM. The high-resolution TEM image of the $Cu_1Mn_2Ce_4$ catalyst is presented in Fig. 4. Several lattice fringes of the crystal structures of Cu and Mn oxides (lattice fringes = 0.253 and 0.187 nm) besides that of CeO_2 (lattice fringes = 0.312 nm) are observed. Therefore, the high activity of the $Cu_1Mn_2Ce_4$ catalyst can be reasonably attributed to its double active structures. One is a mixed structure of Cu and Mn oxides with the function of activating organic molecules. The other one is a ceria-based solid solution structure with the function of transporting active oxygen, including surface and lattice oxygen.

Moreover, the BET surface areas of the catalysts are also listed in Table 1. The surface area of $Cu_1Mn_2Ce_4$ is 45.3 m^2/g, which is higher than that of Cu_1Mn_6 (37.9 m^2/g). However, compared with pure CeO_2 catalyst, the crystallinity of $Cu_1Mn_2Ce_4$ decreases and the average grain size becomes the smallest. This finding indicates that the presence of Cu and Mn in the lattice of CeO_2 results in change to the original phase of the CeO_2 crystalline structure, thereby leading to decreased crystallinity.

2.3. H_2-TPR characterization

Results of TPR analyses for the catalysts are shown in Fig. 5. Cu_1Mn_6 reduction occurs in the form of two peaks at 230°C and 280°C. The peak at a low temperature can be assigned to the reduction of $Cu_{1.5}Mn_{1.5}O_4$; the other one is a shoulder peak associated with the reduction of Mn_3O_4, which can be related to the presence of the Mn_3O_4 and Mn ions with valence lower than +3. When some Mn ions are replaced by Ce, the reduction peaks shift to considerably lower temperatures compared with the Cu_1Mn_6 catalyst. Specifically, the main reduction peaks of $Cu_1Mn_2Ce_4$ and Cu_1Ce_6 sharply shift to 180 and 150°C from 230°C, respectively.

The two reduction peaks of pure CuO normally appear at around 200°C. However, for pure MnO_X, a small reduction peak can be observed at 380°C, which is assigned to the reduction of Mn_3O_4 to MnO (Dai et al., 2012). MnO_X doped with an amount of CuO can effectively promote the reduction of MnO_X, which may be due to two effects: First, CuO has a strong ability of activating the H–H bond, a function common to precious metals. With active H ion overflow occurring, MnO_X reduction occurs. Second, the crystallinity of MnO_X decreases. MnO_X forms lattice defects and oxygen vacancies as a result of CuO doping, which results in enhanced mobility of active oxygen. Morales et al. (2008) milled CuO and Mn_2O_3 to form a mechanical mixed-solid compound and found that CuO does not change the reduction performance of MnO_X. However, after high-temperature calcination, CuO and MnO_X form a new crystalline phase that results in decreased reduction temperature and increased catalytic activity. Therefore, only the interaction between CuO and Mn forming a new crystalline phase can effectively improve their

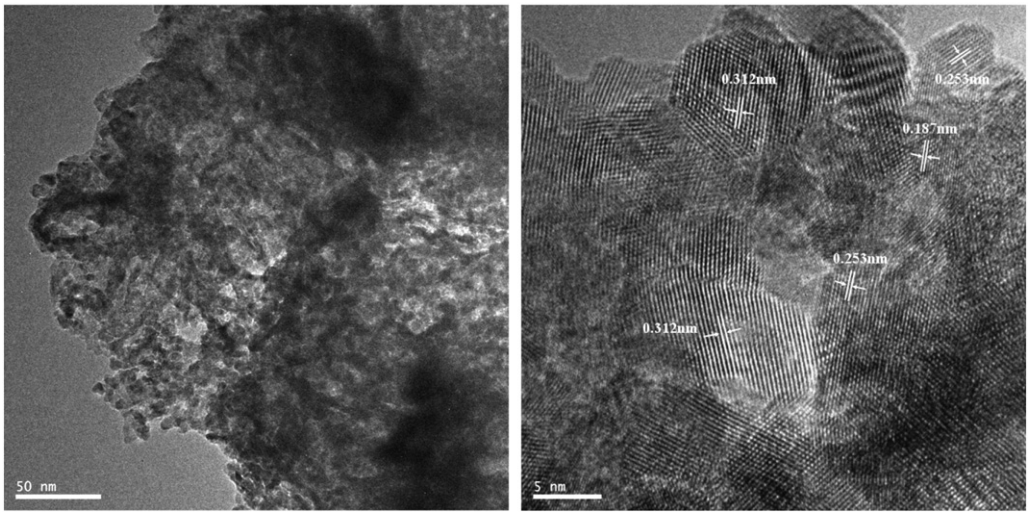

Fig. 4 – HRTEM image of $Cu_1Mn_2Ce_4$ ternary mixed-oxide catalysts.

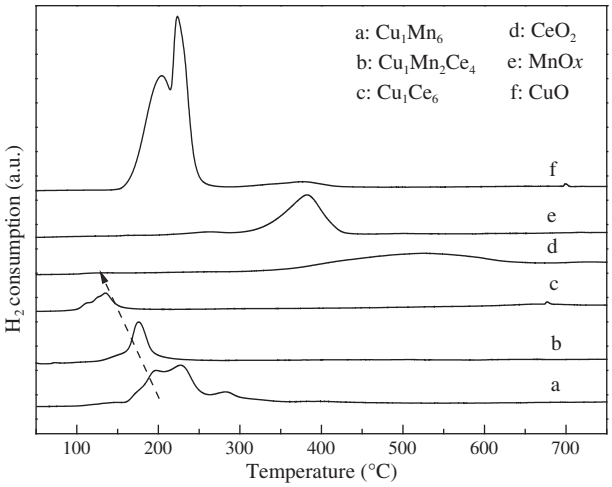

Fig. 5 – H_2-TPR of CeO_2, Cu_1Mn_6, Cu_1Ce_6 and $Cu_1Mn_2Ce_4$ mixed-oxide catalysts.

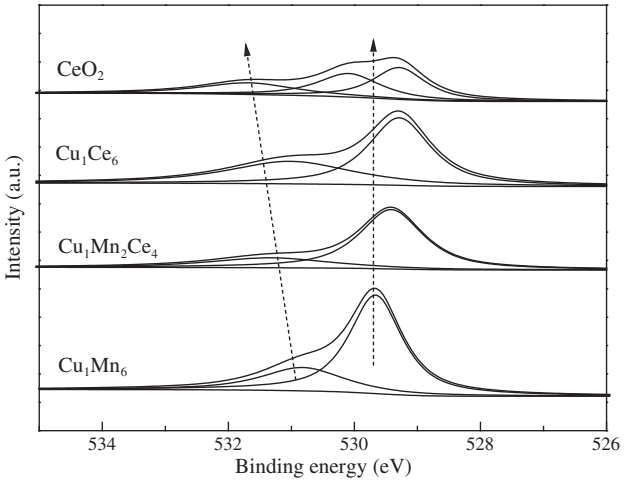

Fig. 6 – XPS spectra of O_{1S} of CeO_2, Cu_1Mn_6, Cu_1Ce_6 and $Cu_1Mn_2Ce_4$ mixed-oxide catalysts.

catalytic oxidation. The second mechanism of lattice defects in Cu–Mn mixed oxides is widely accepted by current researchers.

Considering that Ce is partially substituted for Mn in the catalysts, Cu and Mn ions in the crystalline phase of CeO_2 lead to decreased crystallinity, creating more lattice defects and oxygen vacancies that favor increased oxygen mobility. In addition, the reduction peak of the Cu–Mn–Ce catalyst occurs at lower temperatures compared with the Cu–Mn catalyst, thereby confirming that the defects in the ceria-based solid solution have better oxygen capacity. In addition, The H_2-consumption of the catalysts is listed in Table 1. The H_2-consumption of $Cu_1Mn_2Ce_4$ is 2.32 mmol/g, which is higher than that of Cu_1Ce_6 (1.93 mmol/g); and the H_2-consumption of the Cu_1Mn_6 catalysts is the highest. We propose that the H_2-consumption during reduction directly relates to the oxygen capacity of the catalyst. Namely, the increase of Mn valence is the key factor responsible for the increase of H_2-consumption.

2.4. XPS characterization

The reactive oxygen species located in the mixed-oxide catalysts were characterized by XPS, and the results are shown in Fig. 6. The O_{1s} XPS spectra can be resolved into three peaks (Tang et al., 2006): (1) lattice oxygen (O_{latt}) at 529 to 530 eV; (2) surface oxygen (O_{sur}) at 530 to 532 eV, which is assigned to defect oxides or surface oxygen ions with low coordination and weakly bonded oxygen species; and (3) adsorbed oxygen species (O_{ads}) at 533 to 534 eV from hydroxyl species and adsorbed water species as contaminants on the surface. The peak from 530 to 532 eV corresponds to surface-adsorbed oxygen.

Fig. 6 shows that an increase in the amount of Ce as a substitute for Mn causes an O_{1S} shift to a higher binding energy. The binding energy is 530.9 eV for Cu_1Mn_6 and shifts to 531.6 eV for $Cu_1Mn_2Ce_4$. This result indicates that surface oxygen increases with increased amounts of Ce in the catalysts. Bielanski and Haber (1979) proposed three types of lattice oxygen on the catalyst surface: O_2^{2-}, O^-, and O^{2-}. O_2^{2-} and O^- are electrophilic oxygen species (surface oxygen) that readily participate in excessive and complete oxidation, whereas nucleophilic oxygen species such as O^{2-} (lattice oxygen) mainly play an important role in selective oxidation. The XPS results reveal that the substitution of Ce for Mn in Cu-Mn catalysts can increase the number of electrophilic surface oxygen atoms, thereby effectively promoting the activity for total oxidation.

For $Cu_\chi Mn_{1-\chi}$ (χ = 0.1–0.3) catalysts, the activity improvement was attributed to the presence of the $Cu_{1.5}Mn_{1.5}O_4$ mixed phase and a poorly crystalline manganese oxide, possessing a large amount of oxygen vacancies and lattice defects, which not only create more active oxygen, but also provide the transport channels for active oxygen. $Cu_{1.5}Mn_{1.5}O_4$ serves as the actual active phase and has excellent oxidation capabilities. Crystalline-phase Mn_3O_4 is the center of oxygen supply, with better reducing properties. Based on this theory, the substitution of Ce for Mn in the Cu–Mn catalyst can strongly enhance its redox capabilities. To further improve this catalytic activity, the underlying mechanism was confirmed in our experiment.

For Cu–Mn–Ce ternary oxide catalysts, the formation of a ceria-based solid solution and Cu–Mn oxide active phase with the function of activating organic molecules is the critical factor affecting catalytic combustion at low temperatures. When Ce is partially substituted for Mn, Cu and Mn enter the fluorite-like lattice, leading to the formation of a ceria-based solid solution. Active structures of CeO_2-based solid solutions mainly depend on abundant oxygen vacancies, good oxygen transmission, and increased reduction capability. The CeO_2-based solid solution serves as the oxygen-supplying center with the function of transporting active oxygen, including surface and lattice oxygen. In addition, excess Cu and Mn in Cu–Mn–Ce catalysts are highly dispersed on the surface of CeO_2 as an active phase of Cu–Mn mixed oxides, which has a strong ability to activate organic molecules, thereby serving as the catalyst oxidation center. Therefore, high activity can be reasonably achieved over the $Cu_1Mn_2Ce_4$ catalyst.

3. Conclusions

The partial substitution of Mn by Ce in Cu–Mn catalysts induces a significant change in the structure of the Cu–Mn mixed oxide catalysts. A new ceria-based solid solution phase with the fluorite structure forms, and excess Cu and Mn exist on the surface of the ceria-based solid solution. The CeO_2-based solid solution serves as the oxygen-supplying center with the function of transporting active oxygen, including surface and lattice oxygen. In addition, Cu–Mn mixed oxides are highly dispersed on the surface of CeO_2 as an active phase and can strongly activate organic molecules, thereby serving as the catalyst oxidation center. The resulting structure is highly active for the catalytic combustion of VOCs.

Acknowledgments

We would like to acknowledge the financial support from the Natural Science Foundation of China (No. 21107096), Zhejiang Provincial Natural Science Foundation of China (No. Y14E080008), the Commission of Science and Technology of Zhejiang province (No. 2013C03021), and the Specialized Research Fund for the Doctoral Program of Higher Education (No. 20133317110004).

REFERENCES

Aranda, A., Aylón, E., Solsona, B., Murillo, R., Mastral, A.M., Sellick, D.R., et al., 2012. High activity mesoporous copper doped cerium oxide catalysts for the total oxidation of polyaromatic hydrocarbon pollutant. Chem. Commun. 48 (39), 4704–4706.

Bielanski, A., Haber, J., 1979. Oxygen in catalysis on transition metal oxides. Catal. Rev. Sci. Eng. 19 (1), 1–41.

Dai, Y., Wang, X.Y., Dai, Q.G., Li, D., 2012. Effect of Ce and La on the structure and activity of MnO_x catalyst in catalytic combustion of chlorobenzene. Appl. Catal. B-Environ. 111–112, 141–149.

Du, X.R., Yuan, Z.S., Cao, L., Zhang, C.X., Wang, S.D., 2008. Water gas shift reaction over Cu–Mn mixed oxides catalysts: effects of the third metal. Fuel Proc. Technol. 89 (2), 131–138.

Everaert, K., Baeyens, J., 2004. Catalytic combustion of volatile organic compounds. J. Hazard. Mater. 109 (1-3), 113–139.

Huang, H.F., Liu, Y.Q., Tang, W., Chen, Y.F., 2008. Catalytic activity of nanometer $La_{1-x}Sr_xCoO_3$(x = 0,0.2) perovskites towards VOCs combustion. Catal. Commun. 9 (1), 55–59.

Hutchings, G.J., Mirzaei, A.A., Joyner, R.W., Siddiqui, M.R.H., Taylor, S.H., 1998. Effect of preparation conditions on the catalytic performance of copper manganese oxide. Appl. Catal. A: Gener. 166 (1), 143–152.

Kang, C.H.Y., Kusaba, H., Yahiro, H., Sasaki, K., Teraoka, Y., 2006. Preparation, characterization and electrical property of Mn-doped ceria-based oxides. Solid State Ionics 177 (19-25), 1799–1802.

Liang, Q., Wu, X.D., Weng, D., Xu, H.B., 2008. Oxygen activation on Cu/Mn–Ce mixed oxides and the role in diesel soot oxidation. Catal. Today 139 (1-2), 113–118.

Lu, H.F., Zhou, Y., Huang, H.F., Zhang, B., Chen, Y.F., 2011. *In-situ* synthesis of monolithic Cu–Mn–Ce/cordierite catalysts towards VOCs combustion. J. Rare Earths 29 (9), 855–860.

Lu, H.F., Zhou, Y., Han, W.F., Huang, H.F., Chen, Y.F., 2013a. High thermal stability of ceria-based mixed oxide catalysts supported on ZrO_2 for toluene combustion. Catal. Sci. Technol. 3 (6), 1480–1484.

Lu, H.F., Zhou, Y., Han, W.F., Huang, H.F., Chen, Y.F., 2013b. Promoting effect of ZrO_2 carrier on activity and thermal stability of CeO_2-based oxides catalysts for toluene combustion. Appl. Catal. A: Gener. 464–465, 101–108.

Morales, M.R., Barbero, B.P., Cadús, L.E., 2006. Total oxidation of ethanol and propane over Mn–Cu mixed oxide catalysts. Appl. Catal. B-Environ. 67 (3-4), 229–236.

Morales, M.R., Barbero, B.P., Cadús, L.E., 2008. Evaluation and characterization of Mn–Cu mixed oxide catalysts for ethanol total oxidation: Influence of copper content. Fuel 87 (7), 1177–1186.

Morales, M.R., Barbero, B.P., Lopez, T., Moreno, A., Cadús, L.E., 2009. Evaluation and characterization of Mn–Cu mixed oxide catalysts supported on TiO_2 and ZrO_2 for ethanol total oxidation. Fuel 88 (11), 2122–2129.

Okumura, K., Kobayashi, T., Tanaka, H., Niwa, M., 2003. Toluene combustion over palladium supported on various metal oxide supports. Appl. Catal. B-Environ. 44 (4), 325–331.

Papavasiliou, J., Avgouropoulos, G., Ioannides, T., 2006. *In situ* combustion synthesis of structured Cu–Ce–O and Cu–Mn–O catalysts for the production and purification of hydrogen. Appl. Catal. B-Environ. 66 (3-4), 168–174.

Papavasiliou, J., Avgouropoulos, G., Ioannides, T., 2007. Combined steam reforming of methanol over Cu–Mn spinel oxide catalysts. J. Catal. 251 (1), 7–20.

Parmar, G.R., Rao, N.N., 2009. Emerging control technologies for volatile organic compounds. Crit. Rev. Environ. Sci. Technol. 39 (1), 41–78.

Saqer, S.M., Kondarides, D.I., Verykios, X.E., 2009. Catalytic activity of supported platinum and metal oxide catalysts for toluene oxidation. Top. Catal. 52 (5), 517–527.

Schwartz, W.R., Pfefferle, L.D., 2012. Combustion of methane over palladium-based catalysts: support interactions. J. Phys. Chem. C 116 (15), 8571–8578.

Tanaka, Y., Kikuchi, R., Takeguchi, T., Eguchi, K., 2005. Steam reforming of dimethyl ether over composite catalysts of γ-Al_2O_3 and Cu-based spinel. Appl. Catal. B Environ. 57 (3), 211–222.

Tang, X.F., Li, Y.G., Huang, X.M., Xu, Y.D., Zhu, H.Q., Wang, J.G., et al., 2006. MnO_x–CeO_2 mixed oxide catalysts for complete oxidation of formaldehyde: effect of preparation method and calcination temperature. Appl. Catal. B-Environ. 62 (3-4), 265–273.

Tang, X.F., Xu, Y.D., Shen, W.J., 2008. Promoting effect of copper on the catalytic activity of MnO_x–CeO_2 mixed oxide for complete oxidation of benzene. Chem. Eng. J. 144 (2), 175–180.

Wang, X.Y., Kang, Q., Li, D., 2008. Low-temperature catalytic combustion of chlorobenzene over MnO_x–CeO_2 mixed oxide catalysts. Catal. Commun. 9 (13), 2158–2162.

Zhao, B., Yang, C.Q., Wang, Q.Y., Li, G.F., Zhou, R.X., 2010. Influence of thermal treatment on catalytic performance of Pd/(Ce, Zr)Ox-Al2O3 three-way catalysts. J. Alloys Comp. 494 (1-2), 340–346.

Zimowska, M., Michalik-Zym, A., Janik, R., Machej, T., Gurgul, J., Socha, R.P., et al., 2007. Catalytic combustion of toluene over mixed Cu–Mn oxides. Catal. Today 119 (1-4), 321–326.